

The Evolution of Barium and Europium in Local Dwarf Spheroidal Galaxies

Gustavo A. Lanfranchi¹, Francesca Matteucci² and Gabriele Cescutti²

¹*IAG-USP, R. do Matão 1226, Cidade Universitária, 05508-900 São Paulo, SP, Brazil*

²*Dipartimento di Astronomia-Università di Trieste, Via G. B. Tiepolo 11, 34131 Trieste, Italy*

23 July 2018

ABSTRACT

By means of a detailed chemical evolution model, we follow the evolution of barium and europium in four Local Group Dwarf Spheroidal Galaxies, in order to set constraints on the nucleosynthesis of these elements and on the evolution of this type of galaxies compared with the Milky Way. The model, which is able to reproduce several observed abundance ratios and the present day total mass and gas mass content of these galaxies, adopts up to date nucleosynthesis and takes into account the role played by supernovae of different types (II, Ia) allowing us to follow in detail the evolution of several chemical elements (H, D, He, C, N, O, Mg, Si, S, Ca, Fe, Ba and Eu). By assuming that barium is a neutron capture element produced in low mass AGB stars by s-process but also in massive stars (in the mass range 10 - 30 M_{\odot}) by r-process, during the explosive event of supernovae of type II, and that europium is a pure r-process element synthesized in massive stars also in the range of masses 10 - 30 M_{\odot} , we are able to reproduce the observed [Ba/Fe] and [Eu/Fe] as functions of [Fe/H] in all four galaxies studied. We confirm also the important role played by the very low star formation efficiencies ($\nu = 0.005 - 0.5 \text{ Gyr}^{-1}$) and by the intense galactic winds (6-13 times the star formation rate) in the evolution of these galaxies. These low star formation efficiencies (compared to the one for the Milky Way disc) adopted for the Dwarf Spheroidal Galaxies are the main reason for the differences between the trends of [Ba/Fe] and [Eu/Fe] predicted and observed in these galaxies and in the metal-poor stars of our Galaxy. Finally, we provide predictions for Sagittarius galaxy for which data of only two stars are available.

Key words: stars: abundance – stars: heavy elements – galaxies: abundance ratios – galaxies: Local Group – galaxies: evolution –

1 INTRODUCTION

The proximity and the relative simplicity of the Local Group (LG) Dwarf Spheroidal (dSph) Galaxies make these systems excellent laboratories to test assumptions regarding the nucleosynthesis of chemical elements and theories of galaxy evolution. Several studies addressing the observation of red giants stars in local dSph galaxies with high resolution spectroscopy allow one to infer accurately the abundances of several elements including α -, iron-peak and very heavy elements, such as barium and europium (Smecker-Hane & McWilliam 1999; Bonifacio et al. 2000; Shetrone, Coté & Sargent 2001; Shetrone et al. 2003; Bonifacio et al. 2004; Sadakane et al. 2004; Geisler et al. 2005). These abundances and abundance ratios are not only central ingredients in galactic chemical evolution studies but are also very important in the attempt to clarify some aspects of the processes responsible for the formation of chemical elements.

There is a certain consensus regarding the general aspects of the production of iron peak and α - elements, but for some other elements several questions concerning their production are still open for debate (François et al. 2004). It is largely accepted that α - elements are mainly produced on short time-scales in explosions of type II supernovae (SNe II, Woosley & Weaver 1995; Thielemann, Nomoto & Hashimoto 1996; Nomoto et al. 1997), whereas the iron-peak ones are the main products of type Ia supernovae (SNe Ia, Nomoto et al. 1997), which occur on longer time-scales. The different time-scales involved in these explosions are the main reason for using the ratio between these two sets of elements (the $[\alpha/\text{Fe}]$ ratio) as a cosmic clock, which can be used to impose constraints in the star formation (SF) history of the systems where this ratio is observed (Tinsley 1980; Matteucci 1996). On the other hand, the sites of formation and the processes which are responsible for the production of elements heavier than Fe remain unclear. These elements are synthe-

sized mainly by neutron capture reactions and are normally divided into r-process and s-process elements according to the velocity of the neutron capture reaction, rapid and slow being relative to the duration of the β -decay process, respectively. Among these elements the production of Barium and Europium is more often discussed, due to the characteristics of their formation. They are believed to be produced by the two neutron capture processes in different ways: while Eu is claimed to be a pure r-process element it is believed that the process which dominates the Ba production is the s-process, but with a low fraction of Ba being produced also by the r-process (Wheeler, Sneden & Truran 1989). The stellar mass ranges where these elements are formed are not yet fully understood. The r-process is generally accepted to take place in SNe II explosions (Hill et al. 2002; Cowan et al. 2002). The s-nuclei can be divided into the main component and the weak component elements. The main component elements are synthesized during the thermally pulsing asymptotic giant branch (AGB) phase of low mass stars (Gallino et al. 1998; Busso et al. 2001). A different site is required for the production of the weak component of the s-process elements. These elements are believed to be produced also in advanced evolutionary stages of massive stars (Raiteri et al. 1993).

Models of stellar evolution predict that the main formation (by s-process) of Ba occurs during the thermal pulses of AGB stars with initial masses between 1 to 3 M_{\odot} (Gallino et al. 1998; Busso et al. 2001), with a negligible contribution from intermediate mass stars of ($3 < M < 8M_{\odot}$). As a consequence, the Ba enrichment of the interstellar medium (ISM) due to the s-process is delayed relative to the Fe enrichment, which is produced also in massive stars, and one should expect a low [Ba/Fe] at low metallicities, which would later increase due to the injection of s-processed Ba by the low mass stars (LMS) as [Fe/H] also increases. It has also been suggested that a low fraction of Ba is produced by r-process in stars with masses at the low end of high mass stars ($8 < M < 10M_{\odot}$) (Travaglio et al. 2001), in order to reproduce the [Ba/Fe] ratios observed at low metallicities in the Milky Way. This production would contribute with Ba at early stages of the evolution of the galaxy, prior to the peak of the iron enrichment by SNe Ia.

Europium, on the other hand, is produced only by the r-process which is believed to occur in massive stars ($M > 8M_{\odot}$) (Woosley et al. 1994). The details of the r-process nucleosynthesis remain, however, unclear and several scenarios have been proposed (Woosley et al. 1994; Freiburghaus et al. 1999; Wanajo et al. 2003). Assuming this site of production for Eu, one should observe a relatively high [Eu/Fe] at low metallicities, which would then decrease due to the injection of Fe in the ISM by SNe Ia explosions. However, there is a large spread in the observational data concerning both Eu and Ba in the stars of our Galaxy (Ryan, Norris & Beers 1996; Sneden et al. 1998; Burris et al. 2000), which prevents one from drawing very firm conclusions regarding the production of both Eu and Ba in the Milky Way.

In local dSph galaxies, red giant stars have been observed with high resolution spectroscopy and the abundances of Eu and Ba, among others elements, have been derived (Shetrone, Coté & Sargent 2001; Shetrone et al. 2003; Sadakane et al. 2004; Geisler et al. 2005).

Shetrone, Coté & Sargent (2001) argued that Draco and

Ursa Minor stars exhibit an abundance pattern consistent with one dominated by the r-process, i.e. [Ba/Eu] ranges from solar values at high metallicities to [Ba/Eu] \sim -0.5 at [Fe/H] \leq -1 dex. The pattern of [Ba/Fe] and [Eu/Fe] also resembles the one observed in the halo field stars according to these authors. The same conclusion was reached by Shetrone et al. (2003), who analysed these abundance ratios in Sculptor, Fornax and Carina. Shetrone et al. (2003) claimed also that in Sculptor, Fornax and Leo I the pattern of [Eu/Fe] is consistent with the production of Eu in SNe II.

On the other hand, Venn et al. (2004), pointed out that, despite the general similarity, the dSph stars span a larger range in [Ba/Fe] and [Eu/Fe] ratios at intermediate metallicities than the Galactic stars and, more important, that about half of the dSph stars exhibit lower [Y/Eu] and 2/3 higher [Ba/Y] than the Galactic stars at the same metallicity, thus suggesting a clear difference between the chemical evolution of our Galaxy and the one of dSph galaxies. The [α /Fe] ratios observed in dSphs also are different from the same ratios in the Milky Way showing in general lower [α /Fe] ratios than the Galactic stars with the same [Fe/H] (Smecker-Hane & McWilliam 1999; Bonifacio et al. 2000; Shetrone, Coté & Sargent 2001; Shetrone et al. 2003; Bonifacio et al. 2004; Sadakane et al. 2004; Geisler et al. 2005).

These observations not only shed some light into the chemical evolution history of these galaxies but allowed also the construction of chemical evolution models aimed at reproducing important observational constraints, such as the elemental abundance ratios, the present gas mass and total mass (Carraro et al. 2001; Carigi, Hernandez & Gilmore 2002; Ikuta & Arimoto 2002; Lanfranchi & Matteucci 2003 (LM03); Lanfranchi & Matteucci 2004 (LM04)). Among these models the one proposed by LM03 and LM04 for 6 local dSph galaxies (namely Draco, Carina, Sculptor, Sextan, Ursa Minor and Sagittarius) succeeded in reproducing the observed [α /Fe] ratios, the present gas mass and final total mass by adopting a very low star formation rate, $\nu \sim$ 0.01 to 0.5 Gyr^{-1} (with lower values for Draco and higher ones for Sagittarius) and a high wind efficiency (6-13 times the star formation rate). Besides that, LM04 predicted the stellar metallicity distribution of these galaxies which were later on compared to observational data for Carina with a reasonably good agreement (Koch et al. 2004). The success of LM03 and LM04 models in reproducing several observational constraints allows us to use them as tools to test the theories about the sites of production and the processes responsible for the synthesis of Ba and Eu in dSph galaxies. By adopting the nucleosynthesis prescriptions for these elements which are able to reproduce the most recent observed data for our Galaxy (Cescutti et al. 2005) and comparing the predictions of the models with observational data, it is possible to verify if the assumptions made regarding the nucleosynthesis of Ba and Eu can also fit the data of local dSph galaxies.

The paper is organized as follows: in Sect. 2 we present the observational data concerning the dSph galaxies, in Sect. 3 the adopted chemical evolution models, the star formation and the nucleosynthesis prescriptions are described, in Sect. 4 the predictions of our models are compared to the observational data and the results discussed, and finally in Sect. 5 we draw some conclusions. All elemental abundances are nor-

malized to the solar values ($[X/H] = \log(X/H) - \log(X/H)_\odot$) measured by Grevesse & Sauval (1998).

2 DATA SAMPLE

Recently, red giant stars of dSph galaxies have been the subject of several works with the aim of determining with high-resolution spectroscopy the abundance of several chemical elements including heavy elements such as barium and europium (Bonifacio et al. 2000; Shetrone, Coté & Sargent 2001; Shetrone et al. 2003; Venn et al. 2004; Sadakane et al. 2004; Fullbright, Rich & Castro, 2004; Geisler et al. 2005). From these observations we gathered the data from the galaxies that were analysed in LM03 and LM04 and for which there are abundance determinations for both Ba and Eu. They are Carina, Draco, Sculptor, Ursa Minor and Sagittarius. Despite of the relative small number of data points, it is possible to compare the observed abundance ratios with the model predictions. We choose to compare the observed ratios $[Ba/Fe]$, $[Eu/Fe]$ and $[Ba/Eu]$ with the ones predicted by the models, since these ratios can provide some clues not only to the nucleosynthesis of Ba and Eu, but also to all s-process and r-process elements.

In order to properly compare different data from different authors with the predictions of the models we adopted the abundance values of Shetrone, Coté & Sargent (2001), Shetrone et al. (2003), and Sadakane et al. (2004) updated by Venn et al. (2004). Venn et al. (2004) homogenized the atomica data for spectral lines of Ba and Eu providing data with improved quality which allow a consistent comparison between data from different sources. Otherwise, the effect of combining these different data would be seen as a larger spread in the abundances and possibly in the abundance ratios of 0.1 to 0.2 dex (see Venn et al. 2004). In the case of Bonifacio et al. (2000) data, Eu is obtained using hyper-fine splitting (HFS) (see their Table 5), but Ba is not. The authors claimed that the Ba abundances obtained with HFS would exhibit no significant difference since the line observed (Ba II 6496.9) is a strong line which is not affected by this correction (Bonifacio private communication, see also Shetrone et al. 2003).

Some of the observed stars, however, exhibit anomalous values of $[Ba/H]$ or $[Eu/H]$, and for this reason were excluded from the sample. Two stars in Ursa Minor, K and 199 (in Shetrone, Coté & Sargent 2001), exhibit heavy-element abundance ratios enhanced relative to those typical for other dSph stars: the Ursa Minor K star has an abundance pattern dominated by the s-process and was classified as a Carbon star while Ursa Minor 199 is dominated by r-process (see also Sadakane et al. 2004). In Sculptor, there are also two stars with enhanced heavy-element abundance: Sc982 (Geisler et al. 2005) and Sculptor H-400 (Shetrone et al. 2003). While Shetrone et al. (2003) claimed that the r-process dominated abundance could be attributed to inhomogeneous mixing of the SNe II yields, Geisler et al. (2005) classified Sc982 as a heavy element star which could have been enriched by an other star, which is now dead. Either way, all these stars do not exhibit an abundance pattern characterized only by the nucleosynthesis process occurring inside the star, but also one which was contaminated by external factors. The maintenance of these stars in the sample could lead to an

erroneous comparison with the model predictions and, as a consequence, to a misleading interpretation and to wrong conclusions regarding the processes and the site of production of the heavy elements analysed. Therefore, we excluded these stars from our sample, whereas all the other stars were considered and included in the comparisons with the models predictions.

3 MODELS

We use in this work the same chemical evolution model for dSphs galaxies as described in LM03 and LM04. The model is able to reproduce the $[\alpha/Fe]$ ratios, the present gas mass and the inferred total mass of six dSph galaxies of the Local Group, namely Carina, Draco, Sculptor, Sextan, Sagittarius and Ursa Minor, and also the stellar metallicity distribution of Carina (Koch et al. 2004). The scenario representing these galaxies is characterized by one long episode (two episodes in the case of Carina) of star formation (SF) with very low efficiencies (except in the case of Sagittarius) - $\nu = 0.001$ to 0.5 Gyr^{-1} - and by the occurrence of very intense galactic winds - $w_i = 6-13$. The model allows one to follow in detail the evolution of the abundances of several chemical elements, starting from the matter reprocessed by the stars and restored into the ISM by stellar winds and type II and Ia supernova explosions.

The main features of the model are:

- one zone with instantaneous and complete mixing of gas inside this zone;
- no instantaneous recycling approximation, i.e. the stellar lifetimes are taken into account;
- the evolution of several chemical elements (H, D, He, C, N, O, Mg, Si, S, Ca, Fe, Ba and Eu) is followed in detail;

In the scenario adopted in the previous works, the dSph galaxies form through a continuous and fast infall of pristine gas until a mass of $\sim 10^8 M_\odot$ is accumulated. One crucial feature in the evolution of these galaxies is the occurrence of galactic winds, which develop when the thermal energy of the gas equates its binding energy (Matteucci & Tornambé 1987). This quantity is strongly influenced by assumptions concerning the presence and distribution of dark matter (Matteucci 1992). A diffuse ($R_e/R_d=0.1$, where R_e is the effective radius of the galaxy and R_d is the radius of the dark matter core) but massive ($M_{dark}/M_{Lum} = 10$) dark halo has been assumed for each galaxy.

3.1 Theoretical prescriptions

The evolution in time of the fractional mass of the element i in the gas within a galaxy, G_i , is described by the basic equation:

$$\dot{G}_i = -\psi(t)X_i(t) + R_i(t) + (\dot{G}_i)_{inf} - (\dot{G}_i)_{out} \quad (1)$$

where $G_i(t) = M_g(t)X_i(t)/M_{tot}$ is the gas mass in the form of an element i normalized to a total fixed mass M_{tot} and $G(t) = M_g(t)/M_{tot}$ is the total fractional mass of gas present in the galaxy at the time t . The quantity $X_i(t) = G_i(t)/G(t)$ represents the abundance by mass of an element i , with the summation over all elements in the gas mixture being equal to unity. The star formation rate (SFR),

Table 1. Models for dSph galaxies. $M_{tot}^{initial}$ is the baryonic initial mass of the galaxy, ν is the star-formation efficiency, w_i is the wind efficiency, and n , t and d are the number, time of occurrence and duration of the SF episodes, respectively.

galaxy	$M_{tot}^{initial}(M_{\odot})$	$\nu(Gyr^{-1})$	w_i	n	t(Gyr)	d(Gyr)	IMF
Sculptor	$5 * 10^8$	0.05-0.5	11-15	1	0	7	Salpeter
Draco	$5 * 10^8$	0.005-0.1	6-10	1	6	4	Salpeter
Ursa Minor	$5 * 10^8$	0.05-0.5	8-12	1	0	3	Salpeter
Carina	$5 * 10^8$	0.02-0.4	7-11	2	6/10	3/3	Salpeter
Sagittarius	$5 * 10^8$	1.0-5.0	9-13	1	0	13	Salpeter

i.e. the fractional amount of gas turning into stars per unit time, is given by $\psi(t)$, while the returned fraction of matter in the form of an element i that the stars eject into the ISM through stellar winds and supernova explosions is represented by $R_i(t)$. This term contains all the prescriptions concerning the stellar yields and the supernova progenitor models. The infall of external gas and the galactic winds are accounted for by the two terms $(\dot{G}_i)_{inf}$ and $(\dot{G}_i)_{out}$, respectively. The prescription adopted for the star formation history is the main feature which characterizes the dSph galaxy models.

The SFR $\psi(t)$ has a simple form and is given by:

$$\psi(t) = \nu G(t) \quad (2)$$

where ν is the inverse of the typical time-scale for star formation, the SF efficiency, and is expressed in Gyr^{-1} .

The star formation is not halted even after the onset of the galactic wind but proceeds at a lower rate since a large fraction of the gas ($\sim 10\%$) is carried out of the galaxy. The details of the star formation, such as number of episodes, time of occurrence and duration, are taken from the star formation history of each individual galaxy as inferred by CMDs taken from Dolphin (2002) and Hernandez, Gilmore & Valls-Gabaud (2000). It is generally adopted 1 episode of SF (2 in the case of Carina), with durations which vary from 3 Gyr to 7 Gyr (see Table 1 for more details).

The rate of gas infall is defined as:

$$(\dot{G}_i)_{inf} = Ae^{-t/\tau} \quad (3)$$

with A being a suitable constant and τ the infall time-scale which is assumed to be 0.5 Gyr.

The rate of gas loss via galactic winds for each element i is assumed to be proportional to the star formation rate at the time t :

$$(\dot{G}_i)_{out} = w_i \psi(t) \quad (4)$$

where w_i is a free parameter that regulates the efficiency of the galactic wind. The wind is assumed to be differential, i.e. some elements, in particular the products of SNe Ia, are lost from the galaxy more efficiently than others (Recchi, Matteucci & D’Ercole 2001; Recchi et al. 2002). This fact translates into slightly different values for the w_i corresponding to different elements. Here we will always refer to the maximum value of w_i . It should be pointed out that the differential aspect of the wind has only a small influence on the abundance ratio patterns (including the $[\alpha/Fe]$, $[Ba/Fe]$ and $[Eu/Fe]$ ratios). If, instead, a normal wind (one where all elements are lost with the same efficiency) is used,

the results will not change significantly. The efficiency of the wind, on the other hand, is crucial. It is always high, but different for each dSph galaxy, in order to account for the observational constraints. It is important particularly to reproduce the $[\alpha/Fe]$ ratio, the final total mass and the present gas mass and to define the shape of the predicted stellar metallicity distributions (for more details see LM03 and LM04).

The initial mass function (IMF) is usually assumed to be constant in space and time in all the models and is expressed by the formula:

$$\phi(m) = \phi_0 m^{-(1+x)} \quad (5)$$

where ϕ_0 is a normalization constant. Following LM03 we assume a Salpeter-like IMF (1955) ($x = 1.35$) in the mass range $0.1 - 100M_{\odot}$.

In table 1 we summarize the adopted parameters for the models of dSph galaxies.

3.2 Nucleosynthesis prescriptions

The nucleosynthesis prescriptions are essentially the same as those adopted in LM04, with few modifications. Here we use, as in LM04, Nomoto et al. (1997) for type Ia supernovae, but for massive stars ($M > 10M_{\odot}$) the yields of Woosley & Weaver (1995) are used instead of those from Thielemann, Nomoto & Hashimoto (1996) and Nomoto et al. (1997). This modification does not change the results obtained in the previous papers, and it is based on the best fit to the data of very metal-poor stars of our Galaxy found by François et al. (2004). The only difference is that the predicted $[\alpha/Fe]$ ratios exhibit values somewhat higher, but still in agreement (actually a better one) with the data.

The type Ia SN progenitors are assumed to be white dwarfs in binary systems according to the formalism originally developed by Greggio & Renzini (1983a) and Matteucci & Greggio (1986).

The major difference in the nucleosynthesis prescriptions is the inclusion of the yields of barium and europium in the code, following the procedure adopted by Cescutti et al. (2005), where details can be found.

Barium

We assume two main different processes in the production of barium, taking place in two different sites. The dominant s-process occurring in low mass stars ($1 \leq M/M_{\odot} \leq 3$) and a low fraction of Ba being produced in massive stars through the r-process. The yields from LMS are taken from Busso et al. (2001). The Ba yields resulting from the r-process are assumed to be produced in massive stars in the

Table 2. The stellar yields of massive stars for barium and europium from Cescutti et al. (2005).

$M_{star}(M_{\odot})$	X_{Ba}	X_{Eu}
12.	$9.00 * 10^{-7}$	$4.50 * 10^{-8}$
15.	$3.00 * 10^{-8}$	$3.00 * 10^{-9}$
30.	$1.00 * 10^{-9}$	$5.00 * 10^{-10}$

mass range 10 - 30 M_{\odot} . Travaglio et al. (1999) already predicted production of Ba in massive stars, but in the range 8 - 10 M_{\odot} . Cescutti et al. (2005), on the other hand, showed that the production of Ba in massive stars must be extended to higher masses in order to fully reproduce the most recent observed trend of [Ba/Fe] in Galactic metal-poor stars (François et al. 2005). Following their procedure, we adopted the same yields for the r-processed Ba, which are shown in Table 2.

Europium

The yields of europium are adopted assuming that its production occurs only through the r-process, which takes place in massive stars in a large range of masses (10–30 M_{\odot}). Even though the production of r-process elements is still matter of debate, in Cescutti et al. (2005) a series of models adopting different nucleosynthesis prescriptions for Eu were tested in order to reproduce the trend observed in Galactic metal poor stars. Here we adopted the yields, shown in Table 2, of the model which best reproduced the data, i.e. their model 1.

4 RESULTS

In order to follow the evolution of Ba and Eu in local dSph galaxies and, in this way, to test the adopted nucleosynthesis prescriptions for these two elements we make use of the dSph chemical evolution models from LM03 and LM04 following the procedure and results described there.

In LM03 and LM04, we were able to fit the observed $[\alpha/\text{Fe}]$ ratios and the estimated final total mass and present day gas mass of six local dSph galaxies by varying the most important parameters, such as the SF efficiency and the galactic wind efficiency. The observational constraints were very well reproduced by models adopting very low SF efficiencies ($\nu = 0.005 - 0.5 \text{ Gyr}^{-1}$) and high wind efficiencies ($w_i = 6-13$). These two parameters together are the main responsible for the shape of the observed abundance ratios in dSphs. At low metallicities, at the beginning of the evolution of the system, the $[\alpha/\text{Fe}]$ ratios are relatively high (~ 0.4 dex) due to the almost instantaneous injection of α -elements in the ISM by massive stars which die in the form of SNe II. As the metallicity increases, the $[\alpha/\text{Fe}]$ values start decreasing slowly, and soon after the first explosions of the SNe Ia they go down fast to sub-solar values. This intense decrease after the first SNe Ia explosions is caused by the injection of Fe in the ISM by these explosions and by the occurrence of the galactic wind triggered by them. Since the galactic winds are very intense, with high efficiencies, they remove a large fraction of the gas reservoir which feeds the SF and, consequently, the SFR drops to very low values.

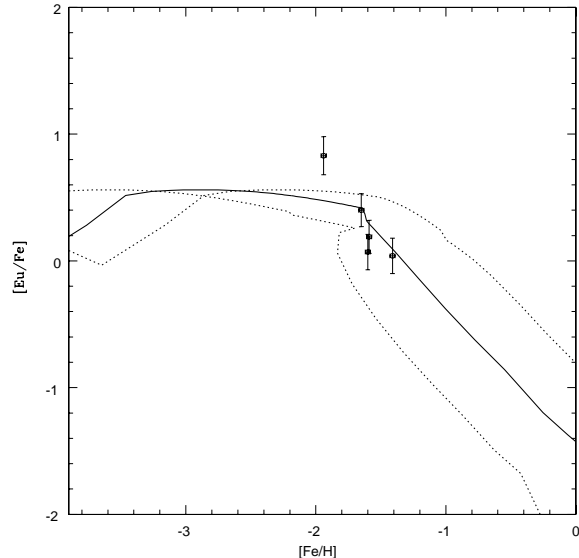


Figure 1. [Eu/Fe] vs. [Fe/H] observed in Carina dSph galaxy compared to the predictions of the chemical evolution model for Carina. The solid line represents the best model ($\nu = 0.1 \text{ Gyr}^{-1}$, $w_i = 7$) and the dotted lines the lower ($\nu = 0.02 \text{ Gyr}^{-1}$) and upper ($\nu = 0.4 \text{ Gyr}^{-1}$) limits for the SF efficiency.

With an almost negligible SF, the injection of α -elements in the ISM is almost halted, whereas the enrichment of Fe proceeds for a very long time (a few Gyr) due to the long lifetime of the stars responsible for its production and injection into the ISM. Consequently, soon after the development of the wind, the predicted $[\alpha/\text{Fe}]$ ratios suffer an abrupt decrease, as it is observed. The final mass and present day gas mass are also controlled by the SF and wind efficiencies: the higher the wind efficiency, the larger the mass of gas lost from the galaxy and the lower the HI gas/total mass ratio. This scenario represents very well the six Local Group dSph galaxies analysed and is able to reproduce the observational data.

Here we adopt the same scenario as described above and the same range of values for the main parameters of the models of LM04 (see table 1 for more details). By means of these models we follow the evolution of Ba and Eu and test the adopted nucleosynthesis prescriptions for these two elements. The predictions of the models are compared with [Ba/Fe], [Eu/Fe] and [Ba/Eu] as functions of [Fe/H].

4.1 Europium

The [Eu/Fe] ratio as a function of [Fe/H] observed in the four Local Group dSph galaxies is compared with the model predictions in the Figures 1 to 4 (Carina, Draco, Sculptor and Ursa Minor, respectively). The predicted behaviour seen in the plots is the same for all galaxies: [Eu/Fe] is almost constant with supra-solar values (~ 0.5 dex) until $[\text{Fe}/\text{H}] \sim -1.7$ dex (depending on the galaxy). Above this metallicity, the [Eu/Fe] values start decreasing fast in Sculptor and Carina (there are no points at these metallicities for Draco and Ursa Minor) similar to what is observed in the case of the $[\alpha/\text{Fe}]$ ratio. This behaviour is consistent with the pro-

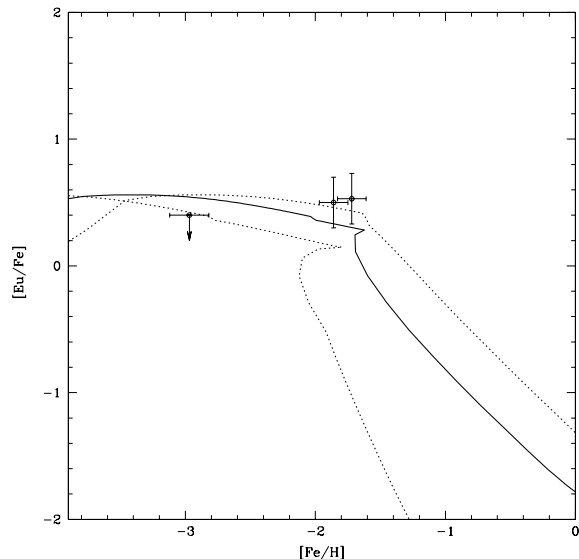


Figure 2. [Eu/Fe] vs. [Fe/H] observed in Draco dSph galaxy compared to the predictions of the chemical evolution model for Draco. The solid line represents the best model ($\nu = 0.03 \text{ Gyr}^{-1}$, $w_i = 6$) and the dotted lines the lower ($\nu = 0.005 \text{ Gyr}^{-1}$) and upper ($\nu = 0.1 \text{ Gyr}^{-1}$) limits for the SF efficiency.

duction of Eu by r-process taking place in massive stars with $M > 10M_{\odot}$. Stars in this mass range have short lifetimes and enrich the ISM at early stages of galactic evolution giving rise to high values of [Eu/Fe], since the production of Fe in these stars is lower than in type Ia SNe occurring later. When the SNe Ia begin to occur, the Fe abundance increases and, consequently, the [Eu/Fe] ratio decreases, as one can see also in the data.

The predicted [Eu/Fe] ratios in all four dSph galaxies well reproduce the observed trend: an almost constant value at low metallicities, and an abrupt decrease starting at $[\text{Fe}/\text{H}] > -1.7$ dex. In the model this decrease is caused not only by the nucleosynthesis prescriptions and stellar lifetimes, but also by the effect of a very intense galactic wind on the star formation rate and, consequently, on the production of the elements involved. In fact, since the wind is very efficient, a large fraction of the gas reservoir is swept from the galaxy. At this point, the SF is almost halted and the production of Eu goes down to negligible values. The injection of Fe in the ISM, on the other hand, continues due to the large lifetimes of the stars responsible for its production. The main result is an abrupt decrease in the [Eu/Fe] ratios, larger than the one that one would expect only from the nucleosynthetic point of view if there was no such intense wind. The abrupt decrease follows the trend of the data very well, especially in the case of Sculptor and Carina. For these two galaxies there are stars observed with metallicities higher than the one corresponding to the time when the wind develops ($[\text{Fe}/\text{H}] > -1.7$ dex), and which are characterized by lower values of [Eu/Fe], in agreement with our predictions. The observed stars of the other two dSph galaxies, Draco and Ursa Minor, exhibit [Fe/H] values which place them before the occurrence of SNe Ia, so it is not possible to verify if the abrupt decrease in the [Eu/Fe] occurs

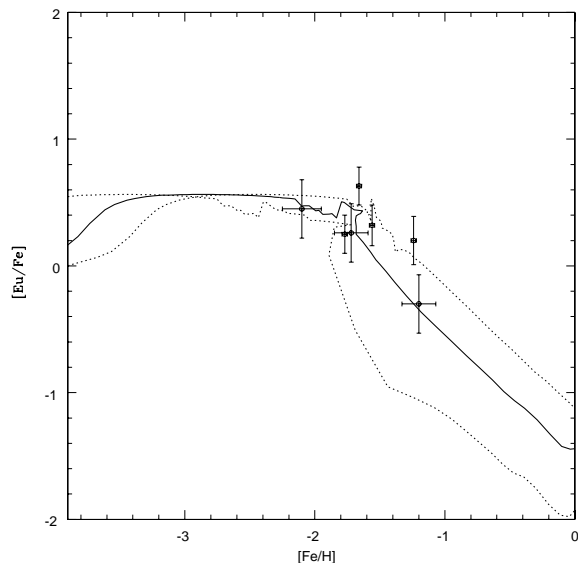


Figure 3. [Eu/Fe] vs. [Fe/H] observed in Sculptor dSph galaxy compared to the predictions of the chemical evolution model for Sculptor. The solid line represents the best model ($\nu = 0.2 \text{ Gyr}^{-1}$, $w_i = 13$) and the dotted lines the lower ($\nu = 0.05 \text{ Gyr}^{-1}$) and upper ($\nu = 0.5 \text{ Gyr}^{-1}$) limits for the SF efficiency.

also in these objects. Only observations of more stars will confirm the trend. It should be said again that the same phenomena explain very well the $[\alpha/\text{Fe}]$ ratios and the final total mass and present day gas mass observed in these galaxies (LM03, LM04).

The small differences in the SF and wind efficiencies do not affect strongly the predictions of the models. As one can see in Table 1, the range of values for the SF efficiency is practically the same for Carina, Sculptor and Ursa Minor ($\nu = 0.02\text{-}0.4$, $0.05\text{-}0.5$, $0.05\text{-}0.5 \text{ Gyr}^{-1}$, respectively), whereas Draco observational constraints are reproduced by a model with lower values of ν , $\nu = 0.005\text{-}0.1 \text{ Gyr}^{-1}$. These values reflect in very similar curves for the first three galaxies and a curve for Draco with only a small difference, namely a [Eu/Fe] ratio which starts decreasing very slowly at metallicities lower ($[\text{Fe}/\text{H}] \sim -2.0$ dex) than in the other three galaxies. However, the abrupt decrease starts at a similar point. The same similarity can be seen in the values of the wind efficiency: Carina - $w_i = 7\text{-}11$, Draco - $w_i = 6\text{-}10$, Sculptor - $w_i = 11\text{-}15$ - and Ursa Minor - $w_i = 8\text{-}12$. Only Sculptor is characterized by a wind efficiency a little bit higher, but this fact does not influence the pattern of the abundances significantly. They all exhibit an intense decrease in the [Eu/Fe] ratio after the wind develops. The small differences in the ranges of values for w_i are related more directly to the gas mass and total mass observed.

What should be highlighted is that the nucleosynthesis prescriptions adopted here allow the models to reproduce very well the data, supporting the assumption that Eu, also in dSph galaxies, is a pure r-process element synthesized in massive stars in the range $M = 10 - 30M_{\odot}$, as it is in the Milky Way (see Cescutti et al. 2005 for a more detailed discussion). Besides that, the low SF efficiencies and the high

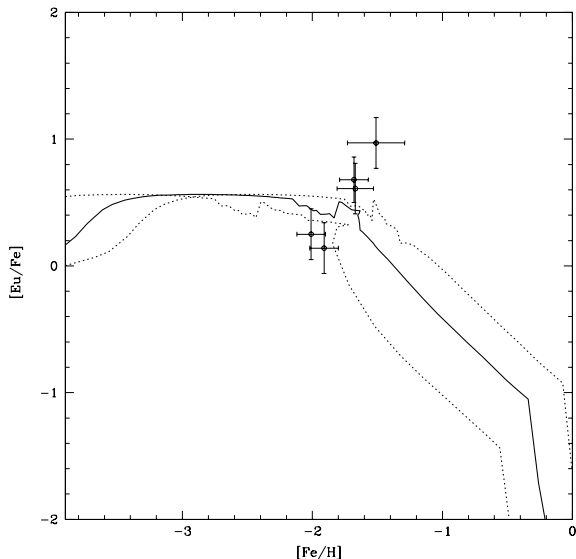


Figure 4. $[\text{Eu}/\text{Fe}]$ vs. $[\text{Fe}/\text{H}]$ observed in Ursa Minor dSph galaxy compared to the predictions of the chemical evolution model for Ursa Minor. The solid line represents the best model ($\nu = 0.2 \text{ Gyr}^{-1}$, $w_i = 10$) and the dotted lines the lower ($\nu = 0.05 \text{ Gyr}^{-1}$) and upper ($\nu = 0.5 \text{ Gyr}^{-1}$) limits for the SF efficiency.

wind efficiencies are required also to explain the $[\text{Eu}/\text{Fe}]$ observed pattern, especially the abrupt decrease of the data in some dSph galaxies.

4.2 Barium

The evolution of $[\text{Ba}/\text{Fe}]$ as a function of $[\text{Fe}/\text{H}]$ predicted by the models and compared to the observed data in four Local Group dSph galaxies is shown in the Figures 5 to 8 (Carina, Draco, Sculptor and Ursa Minor, respectively). One can easily notice that the predicted curves exhibit a similar behaviour in all four galaxies: the predicted $[\text{Ba}/\text{Fe}]$ ratio increases fast at very low metallicities ($[\text{Fe}/\text{H}] < -3.5$ dex), then remains almost constant, close to the solar value, at low-intermediate metallicities ($-3.5 < [\text{Fe}/\text{H}] < -1.7$ dex) and then starts decreasing soon after the occurrence of the galactic wind at relatively high metallicities ($[\text{Fe}/\text{H}] > -1.7$ dex). In this case, the decrease is not so intense as it is in the case of $[\text{Eu}/\text{Fe}]$, due to the differences in the nucleosynthesis of Ba and Eu.

The predicted shape of the $[\text{Ba}/\text{Fe}]$ vs. $[\text{Fe}/\text{H}]$ relation in dSphs can be associated to the two different Ba contributions, from stars in different mass ranges (high masses - 10 to $30 M_{\odot}$ - and low masses - 1 to $3 M_{\odot}$). In the low metallicity portion of the plot the production of Ba is dominated by the r-process taking place in massive stars which have lifetimes in the range from 6 to 25 Myr. Therefore, the $[\text{Ba}/\text{Fe}]$ ratio increases fast reaching values above solar already at $[\text{Fe}/\text{H}] \sim -3.5$ dex and stays almost constant up to $[\text{Fe}/\text{H}] = -1.7$ dex. It is worth noting that the massive star contribution is more clearly seen when the SF efficiency is low. In this regime, in fact, the stars are formed slowly and the difference between the contribution of stars of different

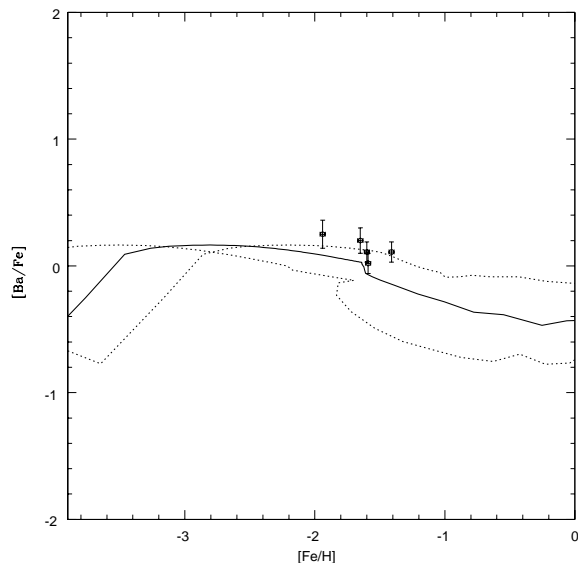


Figure 5. $[\text{Ba}/\text{Fe}]$ vs. $[\text{Fe}/\text{H}]$ observed in Carina dSph galaxy compared to the predictions of the chemical evolution model for Carina. The solid line represents the best model ($\nu = 0.1 \text{ Gyr}^{-1}$, $w_i = 7$) and the dotted lines the lower ($\nu = 0.02 \text{ Gyr}^{-1}$) and upper ($\nu = 0.4 \text{ Gyr}^{-1}$) limits for the SF efficiency.

masses is more evident, since the increase of the metallicity and the evolution of the galaxy proceed at a low speed. On the other hand, when the SF efficiency is higher (like in the Milky Way), the early contribution of massive stars is more difficult to distinguish, because of the much faster increase in metallicity.

At low-intermediate metallicities ($-3.5 < [\text{Fe}/\text{H}] < -1.7$ dex), the production of Ba is still the one by r-process taking place in massive stars, in particular in those with masses around the lower limit for the r-process Ba producers ($\sim 10 M_{\odot}$).

The contribution to s-process Ba enrichment from LMS (lifetimes from 3.8×10^8 years to 10 Gyrs) affects significantly the predicted $[\text{Ba}/\text{Fe}]$ ratio only after the onset of the wind, consequently only after the occurrence of the first SNe Ia. At this stage, the $[\text{Ba}/\text{Fe}]$ starts to decrease rapidly, since the first SNe Ia are injecting large amounts of Fe into the ISM. Together with the enrichment of Fe, the SNe Ia release also large quantities of energy in the ISM which gives rise to a galactic wind. As the galactic wind starts, the SFR goes down to very low values and the production of Ba is limited only to the LMS, especially those at the low mass end. The injection of Ba in the ISM at this stage is, however, not so effective due to the galactic wind which removes a large fraction of the material freshly released in the hot medium (Ferrara & Tolstoy 1999, Recchi et al. 2001, 2004). The effect of the Ba production in LMS is particularly important to slow down the abrupt decrease in $[\text{Ba}/\text{Fe}]$ after the occurrence of the galactic wind. If this production is not taken in account, the $[\text{Ba}/\text{Fe}]$ values after the onset of the wind would go down faster to very low values.

One can see in the Figures 5 to 8 that the observational trends at high metallicities are very well reproduced by the model predictions supporting the assumptions made regard-

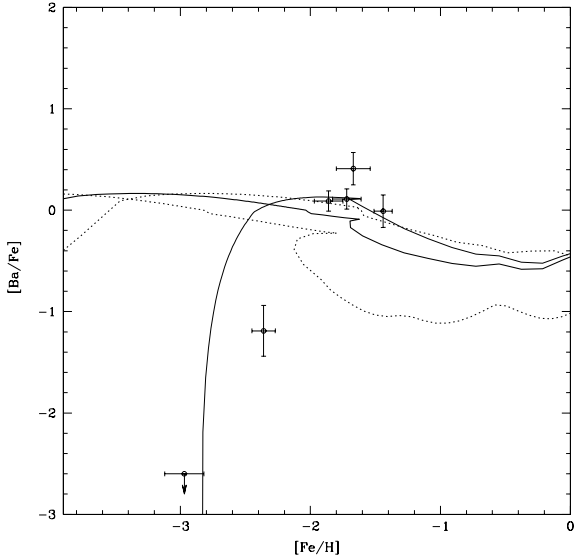


Figure 6. $[\text{Ba}/\text{Fe}]$ vs. $[\text{Fe}/\text{H}]$ observed in Draco dSph galaxy compared to the predictions of the chemical evolution model for Draco. The solid line represents the best model ($\nu = 0.03 \text{ Gyr}^{-1}$, $w_i = 6$) and the dotted lines the lower ($\nu = 0.005 \text{ Gyr}^{-1}$) and upper ($\nu = 0.1 \text{ Gyr}^{-1}$) limits for the SF efficiency. The thin line represents the best model without Ba production in massive stars.

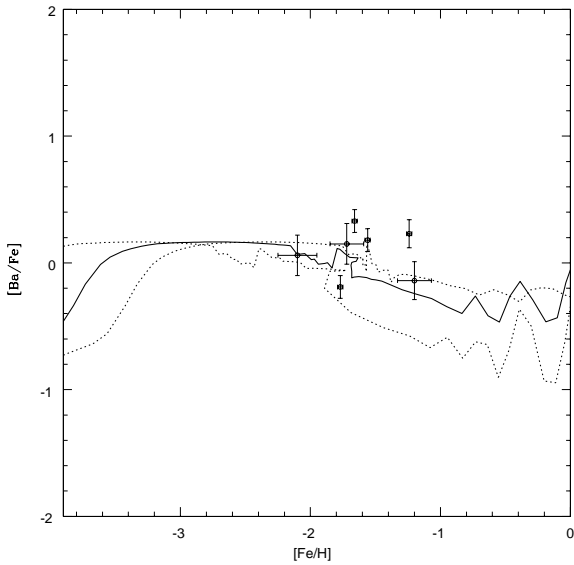


Figure 7. $[\text{Ba}/\text{Fe}]$ vs. $[\text{Fe}/\text{H}]$ observed in Sculptor dSph galaxy compared to the predictions of the chemical evolution model for Sculptor. The solid line represents the best model ($\nu = 0.2 \text{ Gyr}^{-1}$, $w_i = 13$) and the dotted lines the lower ($\nu = 0.05 \text{ Gyr}^{-1}$) and upper ($\nu = 0.5 \text{ Gyr}^{-1}$) limits for the SF efficiency.

ing the nucleosynthesis of Ba. As already mentioned the contribution from LMS to the enrichment of Ba becomes important starting from intermediate to high metallicities ($[\text{Fe}/\text{H}] > -1.9$ dex), depending on the SF efficiency adopted. In this metallicity range, the data of all four galaxies are very well reproduced, including the stars with low values of $[\text{Ba}/\text{Fe}]$ which should have formed soon after the onset of the galactic wind.

On the other hand, at low metallicities ($[\text{Fe}/\text{H}] < -2.4$ dex) only the observational trend of Carina and Sculptor are well fitted by the model predictions. In Ursa Minor and Draco there are a few stars which exhibits a very low $[\text{Ba}/\text{Fe}]$ (~ -1.2 dex) at low $[\text{Fe}/\text{H}]$ (Figures 6 and 8). These points are well below the predicted curves and close to the values of the Milky Way stars at similar metallicities, which are reproduced by a chemical evolution model with the same nucleosynthesis prescriptions adopted here (Cescutti et al. 2005) but with a higher SF efficiency. In general, it seems like if the data for the solar neighbourhood show values of $[\text{Ba}/\text{Fe}]$ lower than in the dSphs at the same metallicity, although this fact should be confirmed by more data. For the α -elements is the opposite, dSph stars show lower $[\alpha/\text{Fe}]$ ratios than Galactic stars at the same metallicity (Shetrone & al. 2001; Tolstoy et al. 2003). LM03 and LM04 suggested that the difference in the behaviour of α -elements in the Milky Way and dSphs should be ascribed to their different SF histories. In particular, the lower $[\alpha/\text{Fe}]$ ratios in dSphs are due to their low star formation efficiency which produces a slow increase of the $[\text{Fe}/\text{H}]$ with the consequence of having the Fe restored by type Ia SNe, and therefore a decrease of the $[\alpha/\text{Fe}]$ ratios, at lower $[\text{Fe}/\text{H}]$ values than in the Milky Way. This effect has been described in Matteucci (2001) and is a consequence of the time-delay model applied to systems with different star formation histories.

Therefore, in the light of what is said above, can we explain also the differences between the predicted $[\text{Ba}/\text{Fe}]$ in dSph galaxies and in the Milky Way? Again, the SF efficiency is the major responsible parameter for this difference. In the Milky Way model the SF efficiency is much larger (10–100 times) than the ones adopted for the dSphs of the sample analysed here. In the low efficiency regime, the contribution from LMS appears at lower metallicities than in the high SF regime, exactly for the same reason discussed for the $[\alpha/\text{Fe}]$ ratios. As a consequence, we predict a longer plateau for the $[\text{Ba}/\text{Fe}]$ ratio in dSphs than in the solar neighbourhood and starting at lower metallicities. This prediction should in the future be confirmed or rejected by more data at low metallicities in dSph galaxies.

Since there are no observed stars at low $[\text{Fe}/\text{H}]$ in Carina and Sculptor while there are three stars (one with an upper limit) with very low $[\text{Ba}/\text{Fe}]$ in Draco and Ursa Minor, one could argue that the Ba production from massive stars is not necessary. To better see the effect of the r-process Ba production from massive stars, we computed models suppressing this contribution. In such a case, the predictions of the models lie below all the observed data and are not capable of fitting the stars with low $[\text{Ba}/\text{Fe}]$. If, on the other hand, besides suppressing the contribution from r-processed Ba synthesised in massive stars one expands the production of s-processed Ba to stars with $M = 3 - 4M_{\odot}$, with an yield $X_{\text{Ba}} = 0.5 \times 10^{-6}$ in this mass range, the models predict a trend similar to that observed (see the thin lines in Figures

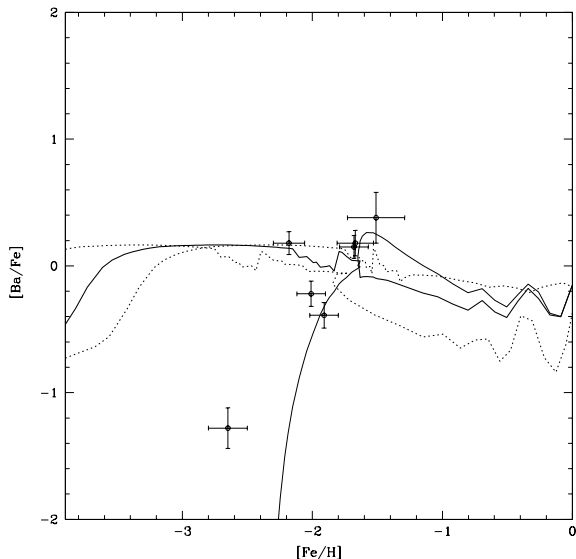


Figure 8. $[\text{Ba}/\text{Fe}]$ vs. $[\text{Fe}/\text{H}]$ observed in Ursa Minor dSph galaxy compared to the predictions of the chemical evolution model for Ursa Minor. The solid line represents the best model ($\nu = 0.2 \text{ Gyr}^{-1}$, $w_i = 10$) and the dotted lines the lower ($\nu = 0.05 \text{ Gyr}^{-1}$) and upper ($\nu = 0.5 \text{ Gyr}^{-1}$) limits for the SF efficiency. The thin line represents the best model without Ba production in massive stars.

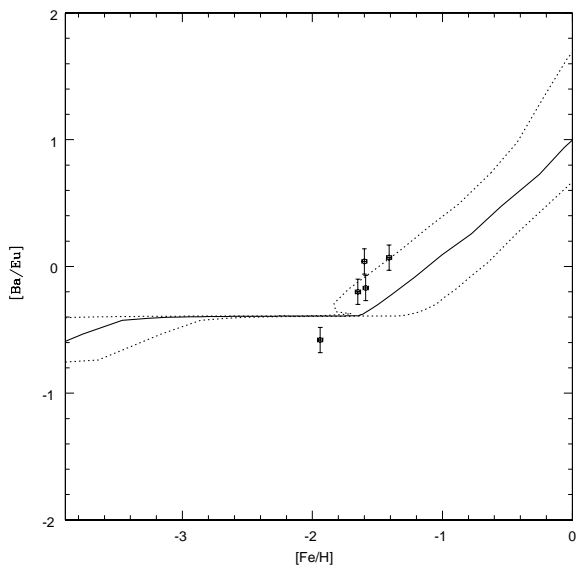


Figure 9. $[\text{Ba}/\text{Eu}]$ vs. $[\text{Fe}/\text{H}]$ observed in Carina dSph galaxy compared to the predictions of the chemical evolution model for Carina. The solid line represents the best model ($\nu = 0.1 \text{ Gyr}^{-1}$, $w_i = 7$) and the dotted lines the lower ($\nu = 0.02 \text{ Gyr}^{-1}$) and upper ($\nu = 0.4 \text{ Gyr}^{-1}$) limits for the SF efficiency.

6 and 8). The assumption of Ba production by s-process in stars with $M = 3 - 4M_{\odot}$ is justified by the fact that this production is predicted by models of stellar evolution (Gallino et al. 1998, Busso et al. 2001), even though there are no such yields available in the literature. Besides that, Travaglio et al. (1999) suggested that the dominant production of Ba comes from stars with $2 - 4M_{\odot}$.

As one can see from the thin lines in Figures 6 and 8, the increase of the $[\text{Ba}/\text{Fe}]$ ratio occurs at metallicities similar to those of the stars with low $[\text{Ba}/\text{Fe}]$. Besides that, this model also reproduces the high values of $[\text{Ba}/\text{Fe}]$ at high metallicities and the $[\text{Ba}/\text{Eu}]$ observed (see next section). In that sense, the observed low values of $[\text{Ba}/\text{Fe}]$, if confirmed by more observations, could be explained by a model with Ba produced only by s-process in stars with masses in the range $M = 1 - 4M_{\odot}$. The problem is that a model with such yields overpredicts the $[\text{Ba}/\text{Fe}]$ at high metallicities in our Galaxy. Consequently, either the production of Ba is not the same in the dSph Galaxies and in the Milky Way, as already suggested by Venn et al. (2004) or these stars are characterised by anomalous metallicities, as others observed in dSph galaxies (see Shetrone et al. 2001; Geisler et al. 2005). Shetrone (2004) analysed the metal poor star Draco 119 (Fulbright, Rich & Castro 2004) which exhibits an upper limit for $[\text{Ba}/\text{Fe}] \sim -2.6$ (an arrow in the Figures 2, 6 and 10) and suggested that this specific star might be contaminated by inhomogeneous mixing, since other stars observed in Draco at similar metallicities present higher values for $[\text{Ba}/\text{Fe}]$ (~ -1.0 dex). These other stars, however, seem to indicate that these low values of $[\text{Ba}/\text{Fe}]$ are not uncommon in Draco and, as a possible consequence, that the production of Ba in Draco (maybe also in other dSph galaxies) is not the same as it is in our Galaxy.

Only more observations of stars with similar metallicities (lower than $[\text{Fe}/\text{H}] \sim -2.0$ dex) in dSph galaxies could solve this problem.

4.3 The ratio $[\text{Ba}/\text{Eu}]$

The comparison between the observed $[\text{Ba}/\text{Eu}]$ as a function of $[\text{Fe}/\text{H}]$ and the predicted curves for the four dSph galaxies is shown in Figures 9 to 12. The models predict a similar pattern for all four galaxies: an almost constant sub-solar value at low metallicities ($[\text{Fe}/\text{H}] < -1.7$ dex) and, after that, a strong increase. This pattern is explained again by the adopted nucleosynthesis and by the effect of the galactic wind on the SFR and, consequently, on the production of Ba and Eu. At the early stages of evolution, the high mass stars provide the major contribution to the enrichment of the ISM medium. Since Ba and Eu are both produced by the r-process taking place in massive stars, they both are injected in the ISM when the gas metallicity is still low. The difference is that Eu is considered to be a pure r-process element, while the fraction of Ba that is produced by the r-process is low and its bulk originates instead from LMS. This fact translates into the sub-solar pattern observed in the predicted curves: more Eu than Ba is injected in the ISM at low metallicities, at an almost constant rate. When the LMS start to die and the first SNe Ia start exploding the scenario changes significantly. The LMS inject a considerable amount of Ba into the ISM causing an increase in the $[\text{Ba}/\text{Eu}]$ ratio. Besides that, the energy released by the SNe Ia contributes

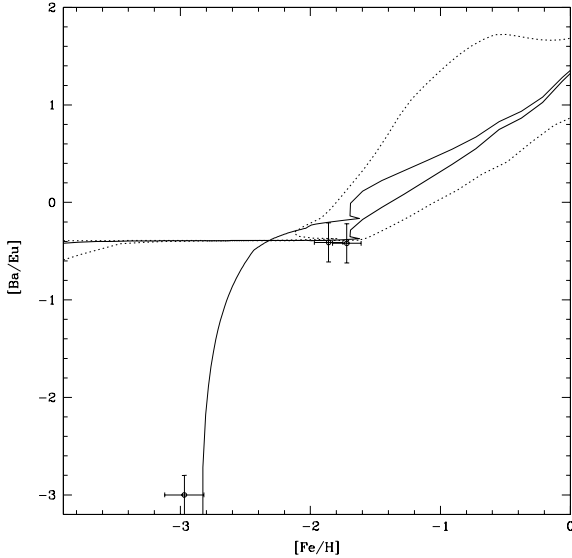


Figure 10. $[\text{Ba}/\text{Eu}]$ vs. $[\text{Fe}/\text{H}]$ observed in Draco dSph galaxy compared to the predictions of the chemical evolution model for Draco. The solid line represents the best model ($\nu = 0.03 \text{ Gyr}^{-1}$, $w_i = 6$) and the dotted lines the lower ($\nu = 0.005 \text{ Gyr}^{-1}$) and upper ($\nu = 0.1 \text{ Gyr}^{-1}$) limits for the SF efficiency. The thin line represents the best model without Ba production in massive stars.

to the onset of the galactic wind. Since the wind is very intense, it removes from the galaxy a large fraction of the gas reservoir which feeds the SF. Consequently, the SFR drops down considerably and also the production of Eu by massive stars, because the number of new formed stars is almost negligible. Barium, on the other hand, continues to be produced and injected in the ISM by the LMS (s-process). This fact induces the increase of $[\text{Ba}/\text{Eu}]$ to be even more intense, as one can see in the predicted curves (Figures 9 to 12).

The observed trend is very well reproduced by the predicted curves in all four galaxies, especially in the case of Carina and Sculptor (Figures 9 and 11, respectively). The abundance pattern of these two galaxies not only exhibits the "plateau" at low metallicities, but also the sudden observed increase of $[\text{Ba}/\text{Eu}]$ after the onset of the wind, suggesting that the adopted nucleosynthesis prescriptions for both Ba and Eu are appropriate and that the scenario described by the chemical evolution models is suitable to explain the evolution of these galaxies. In the case of Draco and Ursa Minor (Figures 10 and 12, respectively), there are no stars with metallicities larger than $[\text{Fe}/\text{H}] \sim -1.7$ dex, the one characteristic for the onset of the galactic wind. Therefore, one cannot verify if this scenario (after the occurrence of the wind) holds also for these systems. However, the "plateau" is very well reproduced, even though there is some dispersion in the data, especially in the case of Ursa Minor.

It is important to stress that the predicted $[\text{Ba}/\text{Eu}]$ reproduces all the observed trends, and that no star, given the uncertainties (with the exception of Draco 119, which exhibits a very uncertain value due to the limits on Ba and Eu abundances), lies outside the predictions, as it was the

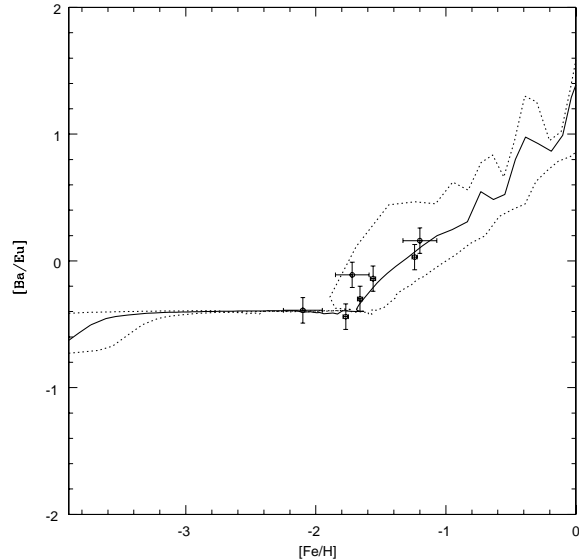


Figure 11. $[\text{Ba}/\text{Eu}]$ vs. $[\text{Fe}/\text{H}]$ observed in Sculptor dSph galaxy compared to the predictions of the chemical evolution model for Sculptor. The solid line represents the best model ($\nu = 0.2 \text{ Gyr}^{-1}$, $w_i = 13$) and the dotted lines the lower ($\nu = 0.05 \text{ Gyr}^{-1}$) and upper ($\nu = 0.5 \text{ Gyr}^{-1}$) limits for the SF efficiency.

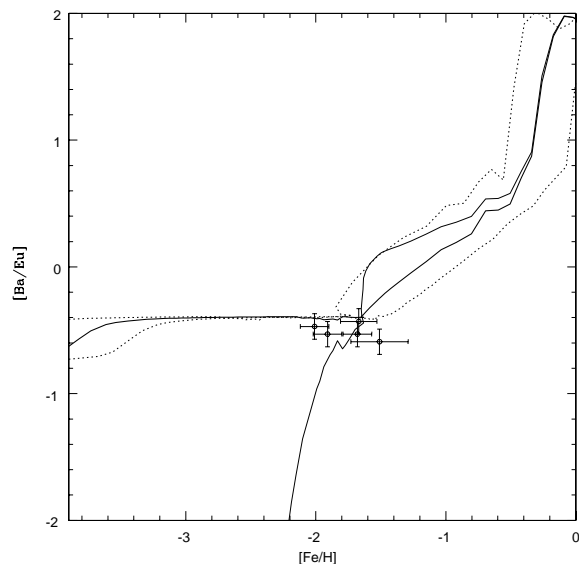


Figure 12. $[\text{Ba}/\text{Eu}]$ vs. $[\text{Fe}/\text{H}]$ observed in Ursa Minor dSph galaxy compared to the predictions of the chemical evolution model for Ursa Minor. The solid line represents the best model ($\nu = 0.2 \text{ Gyr}^{-1}$, $w_i = 10$) and the dotted lines the lower ($\nu = 0.05 \text{ Gyr}^{-1}$) and upper ($\nu = 0.5 \text{ Gyr}^{-1}$) limits for the SF efficiency. The thin line represents the best model without Ba production in massive stars.

case for the two stars with very low $[\text{Ba}/\text{Fe}]$. This fact suggests strongly that the outsider stars must be examined separately.

4.4 The Sagittarius dSph galaxy

In this section, we present the predictions for $[\text{Ba}/\text{Fe}]$, $[\text{Eu}/\text{Fe}]$ and $[\text{Ba}/\text{Eu}]$ as functions of $[\text{Fe}/\text{H}]$ in Sagittarius dSph galaxy. Even though there are only two stars (Bonifacio et al. 2000) observed with Ba and Eu, it is interesting to compare the predictions of the models to the data and to analyse how these ratios would behave in this dSph galaxy. As mentioned in LM04, the Sagittarius dSph galaxy exhibits chemical properties which distinguish this galaxy from the other Local Group dSph galaxies. In particular, the SF efficiency (required to reproduce the observed $[\alpha/\text{Fe}]$ ratios) and the predicted metallicity distribution of this galaxy differ a lot from the other dSph galaxies analysed - Draco, Carina, Ursa Minor, Sextan and Sculptor - being more similar to the values assumed for the Milky Way disc. The required SF efficiency is much higher ($\nu = 1 - 5 \text{ Gyr}^{-1}$ compared to $\nu = 0.01 - 0.5 \text{ Gyr}^{-1}$) and the stellar metallicity distribution exhibits a peak at higher metallicities ($[\text{Fe}/\text{H}] \sim -0.6$ dex) than the other dSph galaxies ($[\text{Fe}/\text{H}] \sim -1.6$ dex) and close to the one from the solar neighborhood. As a consequence, one would expect also $[\text{Ba}/\text{Fe}]$, $[\text{Eu}/\text{Fe}]$ in Sagittarius to be different from the patterns observed in the other four dSph and more similar to those observed in the metal-poor stars of the Milky Way.

In order to predict the evolution of Ba and Eu as functions of Fe, we made use of the Sagittarius dSph model as described in LM04, without any changes in the most important parameters, such as SF efficiency and wind efficiency, and with the same nucleosynthesis prescriptions adopted for the other dSphs. This procedure is justified by the fact that no modifications were required for the LM04 models of the other galaxies (Carina, Draco, Sculptor and Ursa Minor) to fit the observed $[\text{Ba}/\text{Fe}]$, $[\text{Eu}/\text{Fe}]$ and $[\text{Ba}/\text{Eu}]$.

In Figure 13, the predictions for Sagittarius dSph galaxy model for $[\text{Ba}/\text{Fe}]$, $[\text{Eu}/\text{Fe}]$ and $[\text{Ba}/\text{Eu}]$ are shown in comparison with the data. As one can clearly see, all three predicted ratios reproduce very well the data and exhibit significant differences (in particular $[\text{Ba}/\text{Fe}]$) when compared to the predictions (and observations) for the other dSph galaxies. The decrease in the $[\text{Eu}/\text{Fe}]$ at relatively high metallicities ($[\text{Fe}/\text{H}] \sim -1.7$ dex) observed in the four dSph galaxies, and attributed to the effect of the galactic wind on the SFR, is less intense in the case of Sagittarius. Moreover, one cannot see the high values of $[\text{Ba}/\text{Fe}]$ at low metallicities ($[\text{Fe}/\text{H}] < -3.0$ dex), which were explained as an effect of the low SF efficiency. Also, the predicted $[\text{Ba}/\text{Eu}]$ ratios do not show the almost constant "plateau" observed at low and intermediate metallicities in the other dSph galaxies. All these differences can be also found when one compares the pattern of these ratios in dSph galaxies with those in the metal-poor stars of the Milky Way. The differences between the predictions of Sagittarius and the other dSph and the similarities with the Milky Way can be attributed to the high values of the SF efficiency adopted for Sagittarius when compared to the other dSph galaxies. These high values, in fact, are more similar to the values generally adopted for the solar neighborhood (Chiappini, Matteucci & Gratton, 1997).

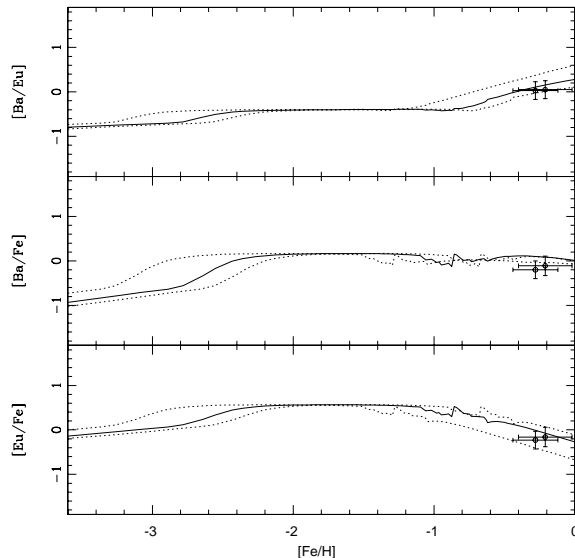


Figure 13. The predicted evolution of Ba and Eu as function of $[\text{Fe}/\text{H}]$ for Sagittarius dSph galaxy compared with the data. The solid line represents the best model ($\nu = 3 \text{ Gyr}^{-1}$, $w_i = 9$) and the dotted lines the lower ($\nu = 1 \text{ Gyr}^{-1}$) and upper ($\nu = 5 \text{ Gyr}^{-1}$) limits for the SF efficiency.

Consequently, one could suggest that the chemical evolution of Sagittarius follows roughly that of the Milky Way disc at the solar neighborhood in contrast to the other dSph Galaxies, which exhibit a much slower chemical evolution.

5 SUMMARY

By means of a chemical evolution model which is able to reproduce several observational constraints of the Local Group dSph galaxies (such as $[\alpha/\text{Fe}]$, present day gas mass, estimated final total mass, metallicity distribution) we followed the evolution of Ba and Eu as a function of Fe in these galaxies in order to verify some assumptions regarding the production of these elements. The model galaxies are specified by the SF prescriptions, such as the number, epoch and duration of the episodes, the SF efficiency and also by the wind efficiency. These two last parameters are the main responsible in defining the shape of the abundance ratio patterns and for the depletion of the gas content of the galaxy. The SF efficiency must be characterised by low values ($\nu = 0.005 - 0.5 \text{ Gyr}^{-1}$) in order to reproduce the observed data whereas the efficiency of the galactic winds must be high ($w_i = 6 - 13$). The effects of a low SF efficiency and an intense wind efficiency on the production of Ba and Eu coupled to the nucleosynthesis prescriptions suggested by Cescutti et al. (2005) and adopted in this work enable us to reproduce very well the observed trends of $[\text{Ba}/\text{Fe}]$, $[\text{Eu}/\text{Fe}]$ and $[\text{Ba}/\text{Eu}]$ as function of $[\text{Fe}/\text{H}]$. This agreement also allowed us to suggest some constraints on the formation and production of Ba and Eu.

The main conclusions can be summarized as follows:

- the observed $[\text{Eu}/\text{Fe}]$ ratio is very well reproduced by the models for all four dSph galaxies with the assumption

that this element is synthesized by r-process in massive stars in a defined range of masses ($10\text{-}30 M_{\odot}$). The pattern of [Eu/Fe] is explained by the different sites of production of these elements, Fe being mainly produced in SNe Ia on long time-scales and Eu in SNe II on short time-scales, and by the effect of the galactic winds on the SFR. At the early stages of evolution the major contributor to the ISM enrichment are the massive stars, giving rise to a high [Eu/Fe] at low [Fe/H] (< -2.0 dex). When the first SNe Ia start exploding and restoring the bulk of Fe then the [Eu/Fe] ratio starts decreasing (time-delay model, Tinsley 1980; Greggio & Renzini 1983b; Matteucci & Greggio 1986; Matteucci 1996). With the energy released by these explosions a galactic wind is triggered and, since it removes a large fraction of the gas reservoir which fuels the SF, the SFR drops down considerably. As a consequence, the enrichment of Eu is almost halted but the one of Fe continues for a long time giving rise to very low values of [Eu/Fe], as observed;

- the predictions of the models for [Ba/Fe] reproduce very well the observed data in all four dSph galaxies with the exception of two stars (one in Draco and another in Ursa Minor) which exhibit very low values of [Ba/Fe] at low metallicities ([Fe/H] < -2.4 dex) and could be anomalous stars. The [Ba/Fe] pattern is explained by the different contributions to the production of Ba and by the effect of the galactic winds on the SFR. Ba is assumed to be produced mainly by s-process in LMS ($1\text{-}3 M_{\odot}$), but also by r-process in massive stars in the range $10 - 30 M_{\odot}$. This last production is more important at early stages of galactic evolution, at low and intermediate metallicities, and is responsible for the high values observed in dSphs at low [Fe/H] and to maintain the predicted [Ba/Fe] almost constant at supra-solar values at intermediate metallicities. The s-processed Ba produced in LMS becomes important later, at higher metallicities ([Fe/H] > -1.9 dex), when the wind develops.

- the low values of [Ba/Fe] at low [Fe/H] observed in Draco and Ursa Minor, if confirmed by more observations, could be explained by a model in which Ba is produced only by s-process occurring in stars with masses in the range $1 - 4 M_{\odot}$. However, this production of Ba is different from the one adopted by a Milky Way model which successfully reproduces the observations (Cescutti et al. 2005). Consequently, if the low values of [Ba/Fe] in dSph galaxies are real, then the production of Ba could be not the same in the dSph galaxies and in the Milky Way. On the other hand, if no other star is observed with such low values, their abundance pattern could be anomalous. This problem could be solved only with more observations of stars in the same metallicity range of the star with reported low [Ba/Fe] ratio;

- the observed [Ba/Eu] as a function of [Fe/H] is very well reproduced by the models with the adopted assumptions regarding the nucleosynthesis of Ba and Eu. The different sites for the production of these elements and the effects of the galactic winds on the SFR are again the main responsables for the pattern observed in [Ba/Eu]. The sub-solar "plateau" at low metallicities is caused by the injection into the ISM of Ba and Eu by massive stars, in different fractions: Eu is assumed to be a pure r-process element, whereas the fraction of r-processed Ba is low. This gives rise to a sub-solar [Ba/Eu]. When the first SNe Ia explode and the wind develops, there is an abrupt change and the [Ba/Eu] suffers

an intense increase, due to the injection in the ISM of Ba by LMS and to the decrease in the SFR. With a very low SFR, the production of Eu is almost halted, but the one of Ba continues since the LMS have a long lifetime (from several 10^8 years to several Gyrs). Therefore, [Ba/Fe] increases considerably, as observed in the dSph stars;

- the nucleosynthesis prescriptions adopted in this work are the same adopted in a chemical evolution model for our Galaxy which reproduces very well the [Ba/Fe], [Eu/Fe] and [Ba/Eu] trends observed in Milky Way (Cescutti et al. 2005). This agreement, coupled to the one achieved here (with red giant stars observed in local dSph galaxies), strongly suggests that the assumptions regarding the formation and production of Ba and Eu are quite reasonable;

- we also compared the data of two observed stars with the predicted evolution of Ba and Eu as functions of Fe in Sagittarius using the same model as described in LM04 and with the same nucleosynthesis prescriptions adopted in this work. The predictions exhibit significant differences when compared to the predictions and observations of the other four dSph galaxies, but similarities to the metal-poor stars of the Milky Way. Both facts can be attributed to the much higher values of SF efficiencies adopted for the Sagittarius galaxy when compared to the other galaxies. This galaxy is much larger and more massive than the other dSphs and could be characterized by a chemical evolution more similar to the one of the solar neighborhood in the Milky Way disc than to the one of the other dSph galaxies;

- finally, we are able to explain the different behaviour of the [Ba/Fe] and [Eu/Fe] in the dSph galaxies and in the Milky Way (here one should place Sagittarius together with the Milky Way instead of with the dSph galaxies). The higher predicted and observed values (although these should be confirmed by more data) of these ratios at low metallicities in dSph galaxies are due to the much less efficient star formation adopted for these galaxies. In this star formation regime, in fact, the metallicity increases more slowly and the different contributions for the Ba enrichment of the ISM appear at lower metallicities than in the Milky Way. For the same reason the $[\alpha/\text{Fe}]$ ratios in dSphs are lower than the same ratios in the Milky Way at the same metallicities, as suggested already by LM03 and LM04.

ACKNOWLEDGMENTS

G.A.L. acknowledges financial support from the Brazilian agency FAPESP (proj. 04/07282-2). F.M. acknowledges financial support from INAF Project "Blue Compact Galaxies: primordial helium and chemical evolution" and from COFIN2003 from the Italian Ministry for Scientific Research (MIUR) project "Chemical Evolution of Galaxies: interpretation of abundances in galaxies and in high-redshift objects".

REFERENCES

- Arimoto N., Yoshii Y., 1987, *A&A*, 173, 23
 Bonifacio P., Hill V., Molaro P., Pasquini L., Di Marcantonio P., Santin P., 2000, *A&A*, 359, 663
 Bonifacio P., Sbordone L., Marconi G., Pasquini L., Hill V., 2004, *A&A*, 414, 503

- Burris D.L., Pilachowski C.A., Armandroff T.E., Sneden C., Cowan J.J., Roe H., 2000, *ApJ*, 544, 302
- Busso M., Gallino R., Lambert D.L., Travaglio C., Smith V.V., 2001, *ApJ*, 557, 802
- Carigi L., Hernandez X., Gilmore G., 2002, *MNRAS*, 334, 117
- Carraro G., Chiosi C., Girardi L., Lia C., 2001, *MNRAS*, 327, 69
- Cescutti G., François P., Matteucci F., Cayrel R., Spite M., Spite F., 2005, *A&A* submitted
- Chiappini C., Matteucci F., Gratton R. 1997, *ApJ*, 477, 765
- Cowan J.J., Sneden C., Burles S., Ivans I.I., Beers T.C., Truran J.W., Lawler J.E., Primas F., Fuller G.M., Pfeiffer B., Kratz K.-L., 2002, *ApJ*, 572, 861
- Dolphin A.E., *MNRAS*, 2002, 332, 91
- François, P.; Matteucci, F.; Cayrel, R.; Spite, M.; Spite, F.; Chiappini, C., 2004, *A&A*, 421, 613
- Freiburghaus C., Rembges J.-F., Rauscher T., Kolbe E., Thielemann F.-K., Kratz K.-L., Pfeiffer B., Cowan J.J., 1999, *ApJ*, 516, 381
- Fulbright, J.P., Rich R.M., Castro S., 2004, *ApJ*, 612, 447
- Gallino R., Arlandini C., Busso M., Lugaro M., Travaglio C., Straniero O., Chieffi A., Limongi M., 1998, *ApJ*, 497, 388
- Geisler D., Smith V.V., Wallerstein G., Gonzalez G., Charbonnel C., 2005, *AJ*, 129, 1428
- Greggio, L., Renzini, A., 1983a, *A&A*, 118, 217
- Greggio, L., Renzini, A., 1983b, in *Frascati Workshop on First Stellar Generations*, Vulcano, Italy, *Societa Astronomica Italiana*, vol. 54, no. 1, p. 311-319
- Grevesse N., Sauval A.J., 1998, *Space Science Reviews*, 85, 161
- Hernandez X., Gilmore G., Valls-Gabaud D., 2000, *MNRAS*, 317, 831
- Hill V., et al., 2002, *A&A*, 387, 560
- Lanfranchi G., Matteucci F., 2003, *MNRAS*, 345, 71
- Lanfranchi G., Matteucci F., 2004, *MNRAS*, 351, 1338
- MacLow M., Ferrara A., 1999, *ApJ*, 513, 142
- Matteucci F., 1992, *ApJ*, 397, 32
- Matteucci F., 1996, *FCPh*, 17, 283
- Matteucci F., Greggio L., 1986, *A&A*, 154, 279
- Matteucci F., Tornambé A., 1987, *A&A*, 185, 51
- Matteucci F., Brocato E., 1990, *ApJ*, 365, 539
- Matteucci F., Romano D., Molaro P., 1999 *A&A*, 341, 458
- Nomoto K., Hashimoto M., Tsujimoto T., Thielemann F.-K., Kishimoto N., Kubo Y., Nakasato N., 1997, *Nucl. Phys. A*, 616, 79
- Raiteri C. M., Gallino R., Busso M., Neuberger D., Kaeppler F., 1993, *ApJ*, 419, 207
- Recchi S., Matteucci F., D'Ercole A., 2001, *MNRAS*, 322, 800
- Recchi S., Matteucci F., D'Ercole A., Tosi M., 2002, *A&A*, 384, 799
- Recchi S., Matteucci F., D'Ercole A., Tosi M., 2004, *A&A*, 426, 37
- Ryan S.G., Norris J.E., Beers T.C., 1996, *ApJ*, 471, 254
- Sadakane K., Arimoto N., Ikuta C., Aoki W., Jablonka P., Tajitsu A., 2004, *PASJ*, 56, 1041
- Salpeter E.E., 1955, *ApJ*, 121, 161
- Schmidt M., 1963, *ApJ*, 137, 758
- Shetrone M., 2004, astro/ph 0411030, to appear in L. Pasquini & S. Randich, eds. *Chemical Abundances and Mixing in Stars in the Milky Way Galaxy and its Satellites*, *ESO Astrophysics Symposia*, Springer-Verlag Press
- Shetrone M., Côté P., Sargent W.L.W., 2001, *ApJ*, 548, 59
- Shetrone M., Venn K.A., Tolstoy E., Primas F., 2003, *AJ*, 125, 684
- Smecker-Hane T., Mc William A., 1999, in Hubeny I. et al., eds. *Spectrophotometric Dating of Stars and Galaxies*, *ASP Conference Proceedings*, Vol. 192, p.150
- Sneden C., Cowan J.J., Burris D.L., Truran J.W., 1998, *ApJ*, 496, 235
- Thielemann F.K., Nomoto K., Hashimoto M., 1996, *ApJ*, 460, 408
- Tinsley B.M., 1980, *FCPh*, 5, 287
- Tolstoy E., Venn K.A., Shetrone M., Primas F., Hill V., Kaufer A., Szeifert T., 2003, *AJ*, 125, 707
- Travaglio C., Galli D., Gallino R., Busso M., Ferrini F., Straniero O., 1999, *ApJ*, 521, 691
- Travaglio C., Galli D., Burkert A., 2001, *ApJ*, 547, 217
- Venn K. A., Irwin M., Shetrone M.D., Tout, C.A., Hill V., Tolstoy E., 2004, *AJ*, 128, 1177
- Wanajo S., Tamamura M., Itoh N., Nomoto K., Ishimaru Y., Beers T.C., Nozawa S., 2003, *ApJ*, 593, 968
- Wheeler J. C., Sneden C., Truran J.W.Jr., 1989, *ARA&A*, 27, 279
- Woosley S.E., Wilson J.R., Mathews G.J., Hoffman R.D., Meyer B.S., 1994, *ApJ*, 433, 229
- Woosley S.E., Weaver T.A., 1995, *ApJS*, 101, 181

This paper has been produced using the Royal Astronomical Society/Blackwell Science L^AT_EX style file.